RSC Advances

ROYAL SOCIETY OF CHEMISTRY

www.rsc.org/advances

SERS-active oligomer Au NR sensor for ultrasensitive detection of mercury ions

Xiaoling Wu[1#], Lijuan Tang[1#], Wei Ma[1], Liguang Xu[1], Liqiang Liu[1], Hua Kuang[1], Chuanlai Xu[1*]

Abstract: In this study, we developed a sensitive Surface-enhanced Raman scattering (SERS) sensor based on a self-assembled Au NR oligomer for the detection of mercury ions (Hg^{2+}) in aqueous solution. Taking advantage of the high sensitivity of Raman spectroscopy and high specificity of the T-Hg^{2+}-T base pair, the method was used in ultratrace analysis of Hg^{2+} in real water samples. The developed Hg^{2+} detection method showed an excellent linear range from 5 to 5000 pM and a limit of detection (LOD) of 4.3 pM (0.86 pg/mL). The recovery experiment presented excellent recovery ranging from 88.98%-105.76%, and demonstrated that the sensor could be used to monitor the concentration of Hg^{2+} for the environmental water.

Keywords: Au NRs, oligomer, Hg^{2+} detection

[1]*State Key Lab of Food Science and Technology, School of Food Science and Technology, Jiangnan University, Wuxi, Jiangsu 214122, China. E-mail: xcl@jiangnan.edu.cn*

[#] These two authors contributed equally to this paper.

1. Introduction

Mercury (Hg) is one of the most toxic heavy metals and can damage the central nervous system and cross the blood–brain barrier by accumulating in the human body.[1] Hg, is an environmental pollutant and is mainly found in drinking water.[2] The biggest threat to humans is the accumulation of Hg ions (Hg^{2+}).[3] Low concentrations of Hg^{2+} can also harm human health. Therefore, there is an urgent need to develop a highly selective and ultrasensitive assay to detect the level of Hg^{2+} in water.

Many traditional quantitative methods have been used for the detection of Hg^{2+}, including inductively coupled plasma mass spectrometry (ICP-MS),[4] cold-vapor atomic fluorescence spectrometry (CV-AFS),[5,6] cold-vapor atomic absorption spectrometry (CV-AAS),[7] and enzyme-linked immunosorbent assay (ELISA).[8] However, most of these methods are of high-cost, labor-intensive and involve complex processes and expensive equipment. Thus, these drawbacks have limited their development. In order to overcome these problems, many new sensors have been developed recently.[9-13] Due to the discovery that Hg^{2+} specifically bridge thymine–thymine (T–T) and form stable and strong T-Hg^{2+}-T base pairs, many novel sensors for Hg^{2+} detection have been developed.[14-16] For example, optical sensors, electrochemiluminescence (ECL) sensors,[17] and electrochemical sensors have been developed for sensitive detection of Hg^{2+}. Furthermore, a Surface-enhanced Raman scattering (SERS) Au NS (gold nanostar) dimer sensor, a fluorescence sensor, and a magnetic resonance imaging sensor were developed by our group.[18]

Recently, the SERS technique, as a quantitative approach, has been extensively used in trace detection.[19-21] Electromagnetic and chemical enhancements are two main effects of increasing the SERS signal. Nanoparticle (NP) assemblies can improve the electromagnetic fields between gaps.[22,23] Our groups have fabricated a variety of

assemblies used in ultrasensitive detection based on this theory. For example, a SERS silver NP (Ag NP) pyramids sensor was used in cancer biomarker analysis,[24] a SERS Au@AgNR dimers sensor was used to detect dopamine,[25] and a SERS heterogeneous core-satellite assembly sensor was used in prostate specific antigen (PSA) detection.[18] Furthermore, our previous studies showed that the chiroptical activity of Au NR oligomers was much higher than that of Au NR dimers[26]. Inspired by these previous studies, we fabricated an ultrasensitive SERS sensor consisting of Au NR oligomers which was applied to the quantitative detection of Hg^{2+} for the enviromental water.

2. Experimental section

2.1 Material

The thiolated DNA aptamer was purchased from Shanghai Sangon Biological Engineering Technology & Services Co., Ltd. (Shanghai, China). The aptamer was purified by high-performance liquid chromatography (HPLC) and suspended in deionized water from a Milli-Q device (18.2 MΩ, Millipore, Molsheim, France). Unless stated otherwise, all chemicals used in this work were purchased from Sigma–Aldrich. Hg^{2+}, Cu^{2+}, Cd^{2+}, Pb^{2+}, Cr^{3+}, Mn^{2+}, Co^{2+}, Fe^{3+}, Zn^{2+}, Al^{3+}, Mg^{2+} (1000 μg/mL in 1% HNO_3 or 5% HCl) were purchased from the National Institute of Metrology (Beijing, P.R China).

The sequences of the oligonucleotides are deliberately designed partly complementary with T-T mismatches[27,28], specific details are as as follows:

DNA1: HS-5'-CCCCCCGTGACCATTTTTGCAGTG-3'

DNA2: HS-5'-CACTGCTTTTTTGGTCACCCCCCC-3'

2.2 Instrumentation

Transmission electron microscopy (TEM) images were obtained using a JEOL JEM-2100 operating at an acceleration voltage of 200 kV. UV-Vis spectra were acquired using a UNICO 2100 PC UV-Vis spectrophotometer and processed with Origin Lab software. Raman spectra were measured using a LabRam-HR800 Micro-Raman spectrometer with Lab-spec 5.0 software attached to a liquid cell. The slit and pinhole were set at 100 and 400 mm, respectively, in the confocal configuration, with a holographic grating (600 g/mm) and an air-cooled He-Ne laser giving 632.8 nm excitation with a power of ~ 8 mW.

2.3 Synthesis of Au NRs

Au NRs were prepared using a seed growth method.[29] 2.5 mL of 0.2 M hexadecyltrimethylammonium bromide (CTAB), 2.375 mL H_2O, and 0.125 mL of 10 mM chloroaurate ($HAuCl_4$) were mixed together, and then 0.3 mL of freshly prepared 0.01 M sodium borohydride (NaBH4) was immediately added. After rapid stirring for 2 min, the color of the solution turned pale brown. Following preparation of the seeds, the Au NRs were fabricated. 5 mL of 0.2 M CTAB solution and 5 mL of 1 mM $HAuCl_4$ were mixed together, and then 0.13 mL of 4 mM $AgNO_3$ was immediately added and left to slowly react for 5 min. Then, 0.07 mL of 0.079 M ascorbic acid (Vc) was added and quickly stirred for 1 min. Finally, 0.012 mL seeds were added, stirred vigorously for 20 s and left at 25°C for 2 h. The reaction was terminated by centrifugation at 7000 rpm for 15 min. 5 mM CTAB solution was then used to resuspend the precipitate to obtain an Au NRs concentration of 1 nM. The final concentration of the as-prepared AuNRs was modified to 1 nM before usage.

2.4 Au NRs modification

The buffer solution used in Au NRs modification was 10 mM Tris. Initially, the end facets of the Au NRs were modified by thiolated PEG1000 (PEG) at a PEG/NR molar ratio of 20:1 to obtain side-by-side oligomers. 50 μL of the prepared Au NRs was mixed with 50 μL buffer solution followed by the addition of 2 μL of 500 nM PEG solution under vigorous stirring. After incubation at room temperature for 8 h, the PEG-modified Au NRs were purified by centrifugation for 5 min at 7000 rpm and washed twice with 100 μL of CTAB. The deposit was collected and resuspended in 100 μL CTAB. The side facets of Au NRs were then modified by thiolated DNA (DNA1/DNA2) at a DNA/NR molar ratio of 80:1. 100 μL of the prepared PEG-modified Au NRs was mixed with 100 μL buffer solution[26]. The 200 μL solution was then divided into two, and 2 μL of 1000 nM DNA1/ DNA2 was added. After modification at room temperature for 8 h, excess DNA was removed by centrifugation (3 times) at 7000 rpm for 5 min each time. The deposit was resuspended in 50 μL of CTAB-Tris buffer.[30]

2.5 Fabrication of the SERS sensor

50 μL of the prepared Au NR-DNA1 and 50 μL of the prepared Au NR-DNA2 were mixed at a molar ratio of 1:1. Then 4-ATP solution was added to achieve a final centration of 10 μM and incubated for 5 h with constant shaking. 1 μL of Hg^{2+} at different concentrations was respectively added to the sensor solutions, resulting in final concentrations of 0, 5, 10, 50, 250, 500, 2500, and 5000 pM. After incubation at 40°C for 1 h, the samples were determined by UV -Vis spectrophotometry, TEM, and SERS.

2.6 Specificity analysis

To evaluate the selectivity of the as-fabricated sensor, ten other metal ions (Cu^{2+}, Cd^{2+}, Pb^{2+}, Cr^{3+}, Mn^{2+}, Co^{2+}, Fe^{3+}, Zn^{2+}, Al^{3+}, Mg^{2+}) were tested at a concentration (500 nM) 100 times greater than that of Hg^{2+} (5 nM). All the other detection procedures were identical to those for Hg^{2+}.

2.7 Analysis of real water samples

Tap water samples (pH=7.2) were taken from Wuxi Water Supply Company and used without purification. Hg^{2+} in the original tap water samples was determined by ICP-MS. Firstly, 2 mg of CTAB was added to 1 mL tap water, and the mixture was shaken for 5 min at 40°C. Next, Au NRs-DNA1/DNA2 was added at the final concentration of 0.25 nM. After adding various concentrations of Hg^{2+} (0, 0.25, 2.5 pM) to the Au NRs/tap water system, the application of this system was verified.[31] While prior to blindly analyze of Tai Lake samples, solid phase extraction was performed to remove potentially interfering substances, and other protocols were exactly the same as the tap water analysis.

3. Results and discussion

3.1 Choice of side-by-side AuNR oligomer and Sensing strategy

Au NR assemblies were intentionally chosen as a SERS substrate in this paper, taking the advantages of more controllable and orderly interface modification and self-assembly (side-by-side or end-to-end) of NRs than NPs[32] (such as Au NP or Ag NP), as well as the continuous and sensitive linear increase of SERS with increasing numbers of NRs. Furthermore, the side-by-side Au NR oligomers were performed

rather than the end-to-end assemblies, due to the higher intensity electric fields (*E*-fields) between the side-by-side AuNR oligomers[26].

As illustrated in Scheme 1, the developed SERS sensor for Hg^{2+} detection was depended on the T-Hg^{2+}-T coordination chemistry[14,16] and partly complementary Au NR-DNA (Au NR-DNA1 and Au NR-DNA2) with deliberately designed T-T mismatches[27,28]. As the Au NR-DNA1 and Au NR-DNA2 were added without Hg^{2+} target, unstable hybridized nanostructures would form at the room temperature, which could completely dissociate by the sharp "melting transitions"[33,34], resulting in the mixture of dispersed AuNR-DNA1 and AuNR-DNA2, therefore the low SERS activity was generated[21,27,28,35]. However, in the presence of Hg^{2+} target, the strong T-Hg^{2+}-T base pairs led to form the stable side-by-side Au NR oligomers without any dissociation under the same conditions, causing the strong SERS activity. Following the addition of different concentrations of Hg^{2+} into the solution containing Au NRs-DNA1 and Au NRs-DNA2, NR oligomers (dimers, trimers and other assemblies) were tended to produce (**Fig. 1**). The composition of the assemblies directly determined the intensity of the SERS signal. With increased Hg^{2+} concentration in the solution, the formation of T-Hg^{2+}-T complexes was enhanced, which led to a gradual increase in the proportion of each aspect of the assemblies (such as dimers, trimers, chains). The solution without added Hg^{2+} was used as a control.

3.2 Analysis of Hg^{2+}

The Au NRs synthesized by the seed growth method had a length and diameter of 42 nm and 14 nm, respectively, with an aspect ratio of 3. In order to obtain the side-by-side Au NR oligomers, the end facets of Au NRs were first blocked by PEG at a PEG/NR molar ratio of 20:1. The side facets of Au NRs were then modified by

DNA1 and DNA2. The molar ratio of DNA/Au NR was optimized. We found that the ratio of 80:1 was optimum. The Au NR assemblies were gradually formed by the addition of Hg^{2+}. The TEM images (**Fig. 1**) show that the Au NRs were assembled with various Hg^{2+} concentrations. It was clearly demonstrated that the complexity and proportion of the assemblies in the presence of 5000 pM Hg^{2+} were much higher than those in the presence of 5 pM Hg^{2+}. When no Hg^{2+} was added, no assemblies were observed. However, in the case of 500 pM Hg^{2+}, a large number of assemblies including trimers, tetramers, and NR chains, but not aggregations were observed. The UV-Vis spectra of Au NRs also changed with the addition of various Hg^{2+} concentrations **(Fig. 2**). The longitudinal surface plasmon peak of Au NR assemblies shifted toward the blue part of the spectrum (from 685 nm to 661 nm) when the Hg^{2+} concentration increased from 0 to 5000 pM. However, the expected blue-shift of the transverse band was too small to be observable, which was probably because that the transverse plasmon dipoles were far apart even when the NRs touched each other[36,37]. The change in UV-Vis spectra was too small for quantitative determination based on the Au NR assembly. However, the Raman intensity of the Au NR assembly markedly changed with the addition of different Hg^{2+} concentrations. Thus, the Au NR oligomers were used as a SERS sensor to detect Hg^{2+}. The characteristic SERS peak of 4-ATP (**Fig. 3a**) at 1080 cm^{-1} (assigned to an in-plane ring breathing mode coupled with vibration of C-S) could be clearly observed in the SERS spectra, and was used to quantify Hg^{2+} in solution. When the Hg^{2+} concentration increased from 0 to 1000 pM, the intensity of the SERS signal at 1080 cm^{-1} increased from 260 to 3200. A standard curve ($y = 252.94 + 941.62lgx$) (**Fig. 3b**) for Hg^{2+} detection was plotted as a function of Hg^{2+} concentration in the range of 5 to 5000 pM, where the SERS intensity (1080 cm^{-1}) was the ordinate. The method displayed a superb correlation with R^2 (regression

coefficient) = 0.991 and the linear range was from 5 to 5000 pM. And the superb linear relation of the raman intensity against the logarithmic concentration of the target was probably due to the exponential increase of the electromagnetic field with the decrease separation between the raman reporter and the "hot spots", which was consistent with the reported studies[24,38,39]. The LOD (limit of detection), which was determined by three times of the standard deviation of the blank solution, was 4.3 pM (0.86 pg/mL), which was higher than that of other methods based on ELISA or instrumental analysis[5,8] and comparable to the method based on the T-Hg^{2+}-T recognition mechanism reported[16,28,31]. And the ultrasensitivity of developed SERS sensor probably should be attributed to the strong plamonic resonance coupling of the side-by-side Au NR oligomer, the sensitive linear response of SERS with increasing numbers of NRs, and the high affinity of T-Hg^{2+}-T mismatch, as well as excellent signal to noise ratio.

3.3 Specificity and selectivity for Hg^{2+}

The selectivity of the as-fabricated sensor for Hg^{2+} detection was evaluated by including the blank control (SERS substrate without any metal ions) and ten other metal ions (Cu^{2+}, Cd^{2+}, Pb^{2+}, Cr^{3+}, Mn^{2+}, Co^{2+}, Fe^{3+}, Zn^{2+}, Al^{3+}, Mg^{2+}). The high affinity and specificity of the T–Hg^{2+}-T complexes resulted in this method having excellent selectivity for Hg^{2+} detection. As illustrated in **Fig. 4**, although the concentration of other metal ions was 100 times higher than Hg^{2+} (5 nM), the SERS signal obtained from Hg^{2+} was much higher than that for the other metal ions. Therefore, this method showed good selectivity.

3.4 Analysis of real water samples

The feasibility of this method was demonstrated by performing recovery experiments using Hg^{2+} spiked tap water samples and Tai Lake water. The Hg^{2+} concentration in the original tap water and Tai Lake water (Wuxi, China), determined by ICP-MS, was 0.27 nM and 1.76 nM, respectively. Hg^{2+} standard solutions were added at a final concentration of 0, 0.25, and 2.5 nM. As shown in **Table 1**, the recovery values for Hg^{2+} were 88.98%-105.76%, indicating that this method showed excellent recovery. Therefore, this method can be used in the detection of Hg^{2+} for the environmental water.

4. Conclusions

In summary, we developed a simple and ultrasensitive SERS sensor platform for the detection of Hg^{2+} in aqueous media based on a self-assembled Au NR oligomer. The LOD for Hg^{2+} detection was 4.3 pM (0.86 pg/mL). The assay was highly sensitive in the detection of Hg^{2+} and was successfully used to detect Hg^{2+} in water. Thus, we believe that this sensor has extensive application in real water sample detection, and show a promising prospect for the environmental monitoring.

Acknowledgements

This work is financially supported by the Key Programs from MOST (2013AA065501, 2012YQ09019410), and grants from Natural Science Foundation of Jiangsu Province, MOF and MOE (BK20140003, 201310128, 201310135).

Notes and references

(1) Kim, H. N.; Ren, W. X.; Kim, J. S.; Yoon, Chem. Soc. Rev. 2012, **41**, 3210.

(2) Wen, S.; Zeng, T.; Liu, L.; Zhao, K.; Zhao, Y.; Liu, X.; Wu, H.-C. *J. Am. Chem. Soc.* 2011, **133**, 18312.

(3) Dave, N.; Chan, M. Y.; Huang, P.-J. J.; Smith, B. D.; Liu, J. *J. Am. Chem. Soc.* 2010, **132**, 12668.

(4) Hong, Y. S.; Rifkin, E.; Bouwer, E. J. *Environ. Sci. Technol.* 2011, **45**, 6429.

(5) Zhang, W.-B.; Yang, X.-A.; Dong, Y.-P.; Xue, J.-J. *Anal. Chem.* 2012, **84**, 9199.

(6) Liu, Z.; Zhu, Z.; Zheng, H.; Hu, S. *Anal. Chem.* 2012, **84**, 10170.

(7) Ghaedi, M.; Reza Fathi, M.; Shokrollahi, A.; Shajarat, F. *Anal. Lett.* 2006, **39**, 1171.

(8) Wang, Y.; Yang, H.; Pschenitza, M.; Niessner, R.; Li, Y.; Knopp, D.; Deng, A. *Anal. Bioanal. Chem.* 2012, **403**, 2519.

(9) Du, Y.; Liu, R.; Liu, B.; Wang, S.; Han, M.-Y.; Zhang, Z. *Anal. Chem.* 2013, **85**, 3160.

(10) Wang, L.; Yao, T.; Shi, S.; Cao, Y.; Sun, W. *Sci. Rep-UK.* 2014, **4**, 5321

(11) Liu, X.; Liu, X.; Tao, M.; Zhang, W. *J. Mater. Chem.* A 2015, DOI: 10.1039/C5TA02491A.

(12) Gao, Y.; Li, X.; Li, Y.; Li, T.; Zhao, Y.; Wu, A. *Chem. Commun.* 2014, **50**, 6447.

(13) Zhu, G.; Li, Y.; Zhang, C.-y. *Chem. Commun.* 2014, **50**, 572.

(14) Ma, Z.-Y.; Pan, J.-B.; Lu, C.-Y.; Zhao, W.-W.; Xu, J.-J.; Chen, H.-Y. *Chem. Commun.* 2014, **50**, 12088.

(15) Pang, Y.; Rong, Z.; Xiao, R.; Wang, S. *Sci. Rep-UK.* 2015, 5, 9451.

(16) Chen, J.; Zhou, S.; Wen, J. *Anal. Chem.* 2014, **86**, 3108.

(17) Zhang, M.; Ge, L.; Ge, S.; Yan, M.; Yu, J.; Huang, J.; Liu, S. *Biosens. Bioelectron.* 2013, **41**, 544.

(18)Ma, W.; Yin, H.; Xu, L.; Wu, X.; Kuang, H.; Wang, L.; Xu, C. *Chem. Commun.* 2014, **50**, 9737.

(19) Lin, E. C.; Fang, J.; Park, S. C.; Stauden, T.; Pezoldt, J.; Jacobs, H. O. *Adv. Mater.* 2013, **25**, 3554.

(20) Mao, H.; Wu, W.; She, D.; Sun, G.; Lv, P.; Xu, J. *Small* 2014, **10**, 127.

(21) Xu, L.; Yin, H.; Ma, W.; Kuang, H.; Wang, L.; Xu, C. *Biosens. Bioelectron.* 2015, **67**, 472.

(22) Zheng, Y.; Thai, T.; Reineck, P.; Qiu, L.; Guo, Y.; Bach, U. *Adv. Funct. Mater.* 2013, **23**, 1519.

(23) Dondapati, S. K.; Sau, T. K.; Hrelescu, C.; Klar, T. A.; Stefani, F. D.; Feldmann, J. *Acs Nano* 2010, **4**, 6318.

(24) Xu, L.; Yan, W.; Ma, W.; Kuang, H.; Wu, X.; Liu, L.; Zhao, Y.; Wang, L.; Xu, C. *Adv. Mater.* 2015, **27**, 1706.

(25) Tang, L.; Li, S.; Han, F.; Liu, L.; Xu, L.; Ma, W.; Kuang, H.; Li, A.; Wang, L.; Xu, C. *Biosens. Bioelectron.* 2015, **71**, 7.

(26) Ma, W.; Kuang, H.; Xu, L.; Ding, L.; Xu, C.; Wang, L.; Kotov, N. A. *Nat. Commun.* 2013, **4**, 2689.

(27) Lee, J.-S.; Han, M. S.; Mirkin, C. A. *Angew. Chem. Int. Ed.* 2007, **46**, 4093.

(28) Ma, W.; Hao, C.; Ma, W.; Xing, C.; Yan, W.; Kuang, H.; Wang, L.; Xu, C. *Chem. Commun.* 2011, **47**, 12503.

(29) Nikoobakht, B.; El-Sayed, M. A. *Chem. Mater.* 2003, **15**, 1957.

(30) Tang, L.; Li, S.; Xu, L.; Kuang, H.; Wang, L.; Xu, C.; Ma, W. *Acs. Appl. Mater. Inter.* 2015, **7**, 12708.

(31) Li, S.; Xu, L.; Ma, W.; Kuang, H.; Wang, L.; Xu, C. *Small* 2015, **28**, 3435

(32) Zhang, L.; Dai, L.; Rong, Y.; Liu, Z.; Tong, D.; Huang, Y.; Chen, T. *Langmuir* 2015, **31**, 1164.

(33) Elghanian, R.; Storhoff, J. J.; Mucic, R. C.; Letsinger, R. L.; Mirkin, C. A. *Science* 1997, **277**, 1078.

(34) Jin, R.; Wu, G.; Li, Z.; Mirkin, C. A.; Schatz, G. C. *J. Am. Chem. Soc.* 2003, **125**, 1643.

(35) Storhoff, J. J.; Elghanian, R.; Mucic, R. C.; Mirkin, C. A.; Letsinger, R. L. *J. Am. Chem. Soc.* 1998, **120**, 1959.

(36)Lee, A.; Andrade, G. F. S.; Ahmed, A.; Souza, M. L.; Coombs, N.; Tumarkin, E.; Liu, K.; Gordon, R.; Brolo, A. G.; Kumacheva, E. *J. Am. Chem. Soc.* 2011, **133**, 7563.

(37) Jain, P. K.; Eustis, S.; El-Sayed, M. A. *J. Phys. Chem. B* 2006, **110**, 18243.

(38) Im, H.; Bantz, K. C.; Lee, S. H.; Johnson, T. W.; Haynes, C. L.; Oh, S.-H. *Adv. Mater.* 2013, **25**, 2678.

(39)Guerrini, L.; Pazos, E.; Penas, C.; Vázquez, M. E.; Mascareñas, J. L.; Alvarez-Puebla, R. A. *J. Am. Chem. Soc.* 2013, **135**, 10314.

Captions:

Scheme 1 Schematic for mercury ion detection based on self-assembled Au NR oligomers

Fig. 1 Representative TEM images of Au NR oligomers assemblies with various Hg^{2+} concentration in the follows: (a) 0; (b) 5 pM; (c) 50 pM; (d) 250 pM; (e) 500 pM; (f) 5000 pM.

Fig. 2 UV-Vis spectra of the sensing systems in the presence of various Hg^{2+} concentration.

Fig. 3 (a) Raman spectrum under different concentrations of Hg^{2+}, and the concentrations of Hg^{2+} were 0, 5, 10, 50, 250, 500 and 2500, 5000 pM; (b) Standard curve of the determination of target Hg^{2+} was plotted with the peak height of the raman signal (I_{1080}) as a functional of logarithmic concentration of the target.

Fig. 4 Evaluation of the selectivity of Raman sensor at different target analytes. The concentration of Hg^{2+} is 5 nM, other analytes' are 500 nM, and blank control was SERS substrate without added any metal ions.

Table 1 Recovery of Hg^{2+} spiked in real water samples

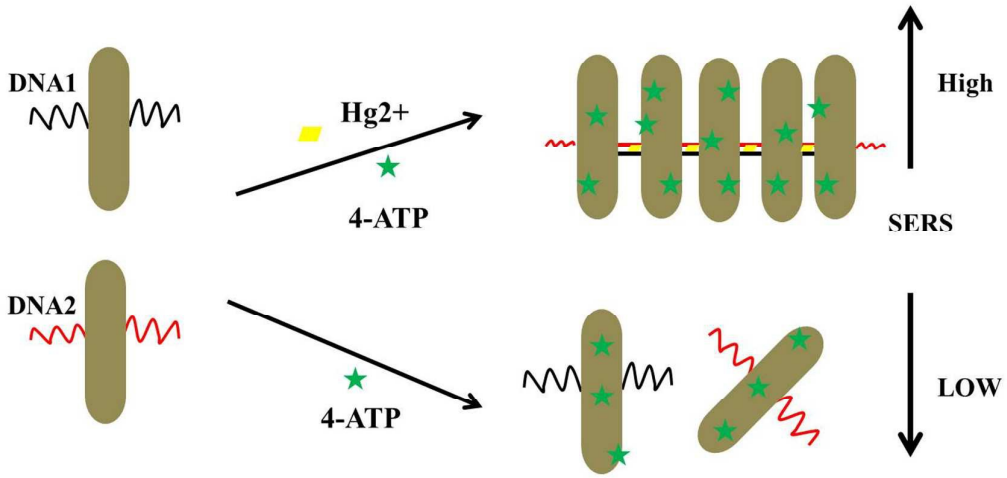

Scheme 1 Schematic for mercury ion detection based on self-assembled Au NR oligomers

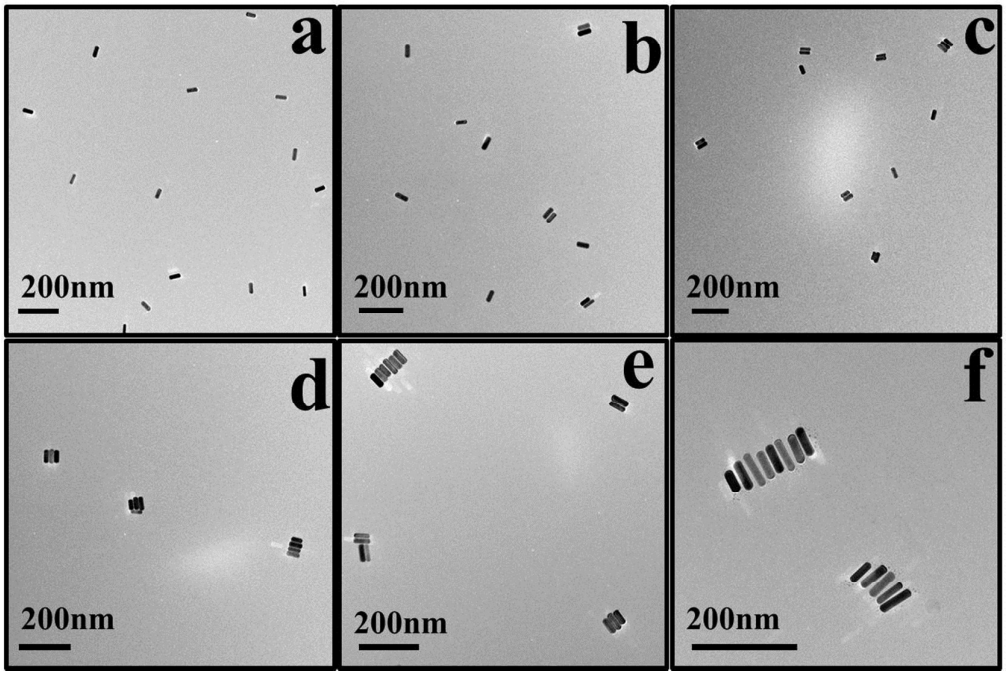

Fig. 1 Representative TEM images of Au NR oligomers assemblies with various Hg^{2+} concentration in the follows: (a) 0; (b) 5 pM; (c) 50 pM; (d) 250 pM; (e) 500 pM; (f) 5000 pM.

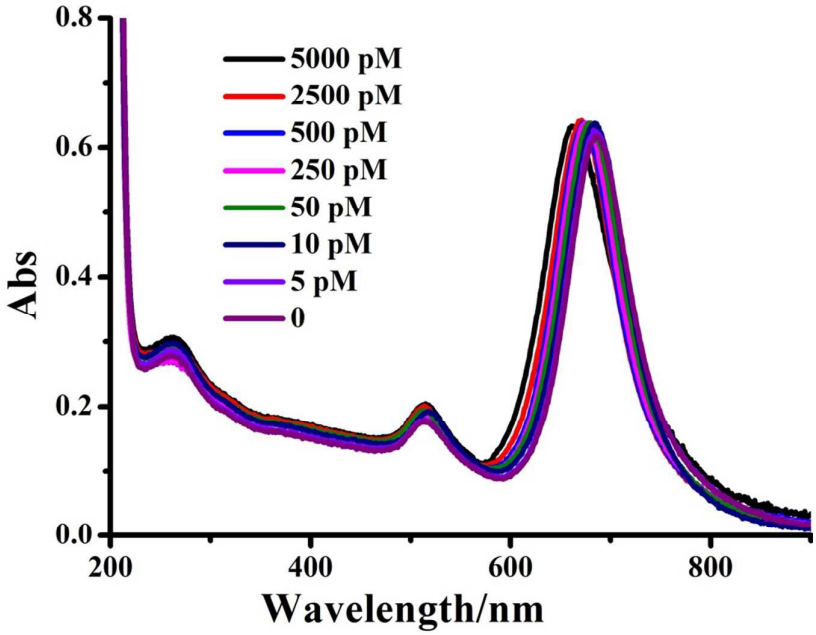

Fig. 2 UV-Vis spectra of the sensing systems in the presence of various Hg^{2+} concentration.

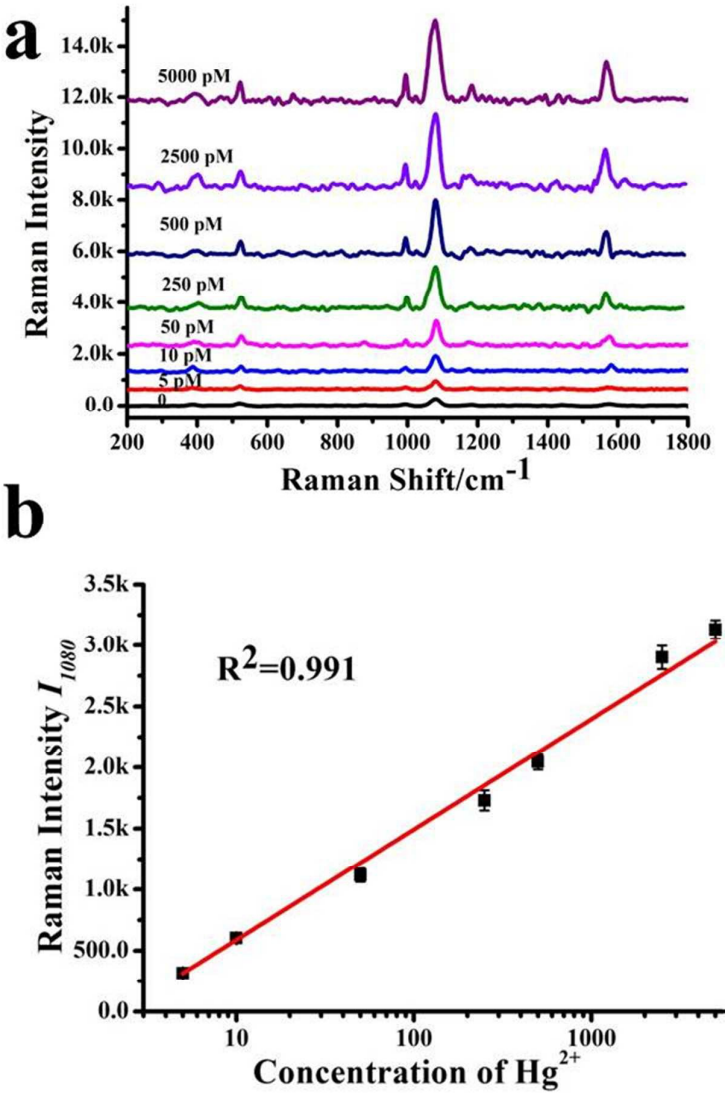

Fig. 3 (a) Raman spectrum under different concentrations of Hg^{2+}, and the concentrations of Hg^{2+} were 0, 5, 10, 50, 250, 500 and 2500, 5000 pM; (b) Standard curve of the determination of target Hg^{2+} was plotted with the peak height of the raman signal (I_{1080}) as a functional of logarithmic concentration of the target.

.

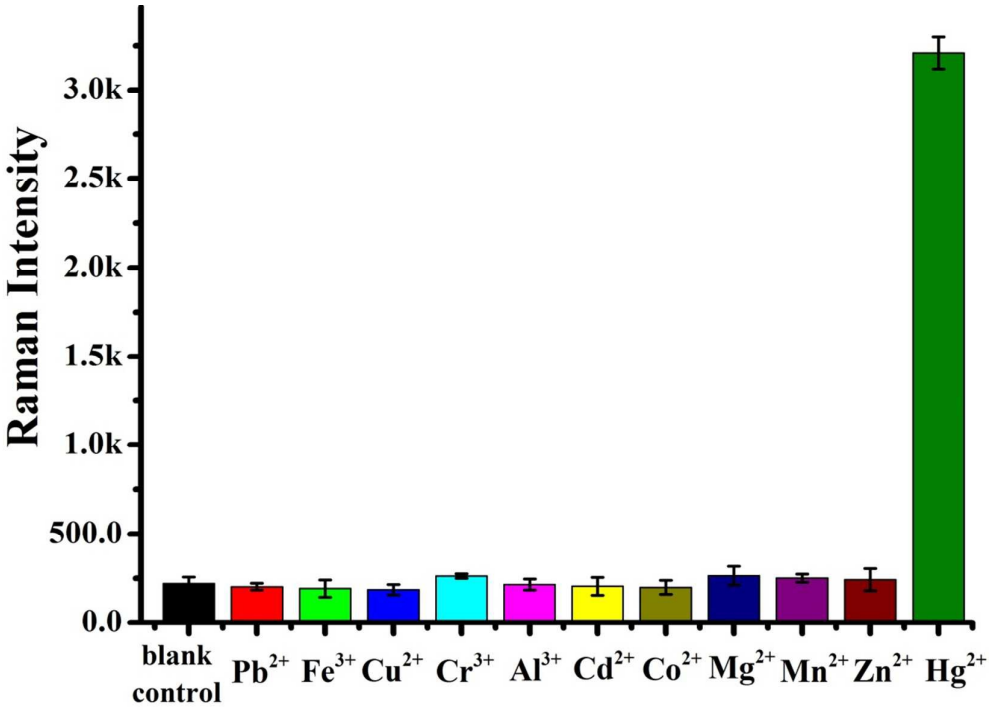

Fig. 4 Evaluation of the selectivity of Raman sensor at different target analytes. The concentration of Hg^{2+} is 5 nM, other analytes' are 500 nM, and blank control was SERS substrate without added any metal ions.

Table 1 Recovery of Hg^{2+} spiked in real water samples

Water Samples[a]	Original Concentration[b] (nM)	Spiked Concentration[c] (nM)	Detected Concentration (Mean±SD[d], nM, n = 5)	Recovery (%) (Mean±SD, n = 5)
Tap water	0.27	0	0.24±0.07	88.89±25.9
	0.27	0.25	0.55±0.09	105.76±17.3
	0.27	2.5	2.66±0.35	96.03±12.5
Water from Tai Lake	1.76	0	1.68±0.11	95.45±13.4
	1.76	0.25	1.87±0.16	93.03±15.7
	1.76	2.5	3.82±0.36	89.67±19.5

[a] The water samples were sampling from the original tap water and Tai Lake water (Wuxi, China)

[b] 100x concentrated Hg^{2+} of the original tap water and Tai Lake water (Wuxi, China) were determined by inductively coupled plasma-mass spectrometry (ICP-MS). Prior to blindly analyze, the Tai Lake samples were extracted by solid phase extraction to remove potentially interfering substances.

[c] Different spiked concentration of Hg^{2+} was prepared from diluting the thawed 500 nM Hg^{2+} standards (determined by ICP-MS) with tap water and Tai Lake water.

[d] SD was calculated based on five parallel experiments for each sample.